Journal of Applied Fluid Mechanics, Vol. 9, No. 6, pp. 3061-3071, 2016.
Available online at www.jafmonline.net, ISSN 1735-3572, EISSN 1735-3645.
DOI: 10.29252/jafm.09.06.26098

On the Effect of Aspect Ratio of Open Heated Channel Including an Active Obstacle upon the Turbulent Characteristics of a Thermal Plume: Experimental Analysis

T. Naffouti [1,2†], J. Zinoubi [1,2] and R. B. Maad [1]

[1] *Université Tunis El-Manar, Faculté des Sciences de Tunis, Département de Physique, Laboratoire d'Energétique et des Transferts Thermique et Massique, El Manar 2092, Tunis, Tunisia.*
[2]*Université Tunis El-Manar, Institut Préparatoire aux Etudes d'Ingénieurs El-Manar, El-Manar 2092, Tunis, Tunisia.*

†*Corresponding Author Email: taoufiknaffouti@gmail.com*

(Received January 11, 2016; accepted April 29, 2016)

ABSTRACT

This paper reports an experimental investigation of aspect ratio effect of open vertical channel on turbulent characteristics of a thermal plume. The physical configuration is constituted essentially by a prallelepipedic channel and an obstacle of a rectangular section. The thermal plume is generated by a rectangular obstacle heated uniformly at the upper surface. This active source is placed at the entry of a vertical channel open at the ends. The symmetrical heating of channel walls by joule effect and by thermal radiation emitted by the plume, causes the appearance of a thermosiphon flow which interacts with this one. To investigate the flow fluctuations, an anemometer at constant current (CCA) is used. The results carried out with air (Pr = 0.71) are performed for Rayleigh number equal to 0.63 10^7 over a wide range of aspect ratio $1.25 \leq A \leq 30$. Effects of this pertinent parameter are displayed upon thermal and dynamic turbulent fields. Using Taylor hypothesis, time and length scales of turbulent thermal field are studied. It is found that the turbulent characteristics of the flow are significantly influenced by the variation of aspect ratio. An optimum aspect ratio of channel characterized by a strong homogenization of turbulence of the flow is observed. The fine analysis of temperature fluctuations spectra shows the evolution of the vortices in energy cascade owing to the strong effect of thermosiphon flow which favours the vortex stretching.

Keywords: Thermal plume; Thermosiphon flow; Turbulence scales; Power spectral density; Spectral laws; Optimum aspect ratio.

NOMENCLATURE

A	aspect ratio of channel	F_{ad}	dynamic flatness factor,
b_1	source width	F_{dt}	thermal skewness factor,
D_f	sensitive wire diameter	F_{dd}	dynamic skewness factor
e	spacing between channel walls	g	gravitational acceleration
E	energy spectral density	L_E^*	dimensionless of length scale of the dimensionless length scale of the thermal turbulence
E*	dimensionless energy spectral density		
F_{at}	thermal flatness factor		
I_t	thermal turbulent intensity of the flow	U	vertical average component velocity of the flow
I_d	dynamic turbulent intensity of the flow		
L_2	height of the channel	U_0	reference velocity,
L_1	length of the source	U'	vertical component velocity fluctuating of the flow
L_2	length of the channel		
L_f	length of the sensitive wire	(x,y,z)	Cartesian coordinates
n	frequency	X*	dimensionless coordinate,
Ra	Rayleigh number	Z*	dimensionless height
T	average temperature		

T_a	temperature of the ambient air
T_s	temperature of the hot source
T'	temperature fluctuation
T_E	time scale of the thermal turbulence
T_E^*	dimensionless time scale of the thermal turbulence
L_E	length scale of the thermal turbulence
β	thermal expansion coefficient
τ	time shift
ν	kinematic fluid viscosity
χ	thermal diffusivity

1. INTRODUCTION

The physical phenomenon of turbulent thermal plumes evolving in free or confined medium have been extensively investigated both experimentally and numerically owing to its several applications in nature and in industry, such as fires in forests/buildings/corridors, effect chimney, solar collectors, electronic components (McGrattan *et al*., 1996; Inard *et al*., 1997; Baum *et al*., 1998; Shiraishi *et al*., 1998; Zinoubi *et al*., 2004; Lavrov *et al*., 2006; Porterie *et al*., 2007; Yucel *et al*., 2008; Shi *et al*., 2009; Wang *et al*., 2009; Lee *et al*., 2010; Naffouti and Djebali, 2012; Naffouti *et al*., 2013; Rahmani *et al*., 2013; Li *et al*, 2014; Naffouti *et al*., 2015). Analysis of this natural convection flow presents a crucial importance to develop the techniques of prevention, to optimize the convective heat transfer of thermal systems and to better control the fires.

Most investigations related to thermal plumes flows in free and confined mediums are focused on the thermal and dynamic characteristics in physical space. By studying the buckling of a thermal plume, Yang (1992) noted that the transition region from laminar to turbulent flow is characterized by an asymmetrical deformation. Then, Dehmani *et al*. (1996) performed an experimental investigation on turbulent structure of axisymmetric thermal plume penetrating strong density stratification. It is found that the buoyancy forces are dominant in the zone of plume. Ouled Mohamed Mahmoud *et al*. (1998) studied a thermal plume generated by a hot disc heated uniformly at 573 K. After that, Elicer-Cortes *et al*. (1999) experimentally studied the ultrasound scattering from a turbulent round thermal pure plume. A numerical simulation was made by Haraa *et al*. (2004) on thermal plumes in free space using the $k-\varepsilon$ standard model. By analyzing the development of a turbulent thermal plume produced by a turning hot disc, Pham *et al*. (2006) showed an amplification of thermal and dynamic turbulent intensity rates as increasing the disc rotation. Then, Naffouti *et al*. (2010) characterized the turbulent structure of a free thermal plume generated by a rectangular hot source. It is found that the fluctuating field is divided in two zones.

Many contributions are focused on the interaction phenomenon of a thermal plume with wall/thermal plume/thermosiphon flow. Agator (1983) made an experimental study on the interaction of a thermal plume produced by a spherical calotte heated at 737 K, with a vertical wall. Two zones of the flow and a destruction of the symmetry of thermal turbulence intensity plots are concluded. Then, Brahimi (1987, 1989) analyzed the interaction of two identical turbulent thermal plumes generated by two hot discs. It is found a strong interference between the plumes. A. Ould Mohamed Mahmoud (1998) analyzed the thermal plume in a vertical cylinder open at the ends. Near the active source, a supplementary instability zone is added to classical zones. By studying the same configuration, Zinoubi *et al*. (2004) are interested to form factor effects on the resulting flow of plume-thermosiphon. Bouslimi *et al*. (2005) studied a guided turbulent thermal plume by a vertical cylinder open at the ends. Next, Zinoubi *et al*. (2007) studied a turbulent thermal plume with heat disc inside a vertical prallelepipedic canal. Using lattice Boltzmann method, a numerical study of thermal plumes at high Rayleigh number has been conducted by Rosdzimin *et al*. (2010). It is shown that the movement of thermal plumes is influenced by the distance between two heated cylinders. T. Naffouti *et al*. (2009) experimentally studied a turbulent thermal plume inside a vertical canal heated by thermal radiation. The results show that the turbulent structure of the flow is divided in three zones. Recently, Naffouti *et al*. (2015) analyzed the effect of spacing between canal walls maintained at a constant temperature of 323 K on the thermal and dynamic average fields of a turbulent thermal plume. It is found the existence of an optimum spacing whose flow rate and thermal energy are maxima.

In order to estimate the average length and time of the vortices structures of the flow, a limited number of investigations are oriented to study the turbulence characteristics scales. Agator *et al*. (1983) experimentally investigated the thermal turbulent field of a thermal plume generated by a hot spherical calotte. The flow is characterized by a big length scale on the plume axis about 22.1 cm. In addition, it is found that this scale loses half of its value when an obstacle is located in the immediate vicinity of the plume such as a vertical plate or a second identical plume. For a vertical isotherm plane plate (1978), the longitudinal length scale of turbulence does not exceed 10 cm. By studying the length scale of dynamic turbulent field of thermal plume evolving in a stratified medium, Dehmani *et al*. (1996) show that the dissipative vortices average length is approximately 0.9 cm. Compared to the results of Son (1977), dissipation scale is about a centimeter.

Few researchers contributed to spectral analysis of thermal plume fluctuations. Agator *et al*. (1983) show a shift of the spectra of a thermal plume by a hot spherical calotte towards high frequency as we move away from the active source. Dehmani *et al*.

(1996) studied the axial evolution of the spectra of dynamic fluctuations of thermal plume penetrating strong density stratification. It is noted that the production effects by "buoyancy" are identified in the zone of the plume corresponding to the law n^{-1} of Tchen (1953). After that, an experimental study was conducted by Elicer-Cortés *et al*. (2004) on the thermal spectra from a turbulent thermal plume by ultrasound scattering. It identified three distinct spectral laws versus the frequency n. A first region of energy production characterized by the law n^2. A third region of energy dissipation where the law n^{-7} of Heisenberg (1983) is identified. An intermediate region of energy transfer from the largest vortices towards the smallest scales where the law n^{-3} of Lumley (1964) is observed. This law is characteristic of anisotropic turbulence caused by the buoyancy forces (2002). By studying the temperature fluctuations spectra of a resulting flow plume-thermosiphon in a vertical canal heated only by thermal radiation, Naffouti *et al*. (2009, 2010) show that the big structures vortices carriers of energy evolve toward smaller dissipative structures as we move away from the active source. After that, Zinoubi *et al*. (2011) examined the thermal spectra of a thermal plume generated by a hot disc placed at the entry of a vertical prallelepipedic canal. He showed the existence of the laws spectral n^{-1}, n^{-3} and n^{-7}.

The present analysis represents a further effort to extend the experimental study carried out by Naffouti *et al*. (2015) on the effect of walls spacing of a vertical channel on thermal and dynamic average fields of a thermal plume. This investigation has not been concerned with the effect of aspect ratio of a vertical channel on turbulent characteristics of a thermal plume generated by an active obstacle. Hence, the main objective of this study is to release the effect of aspect ratio of a vertical channel heated at a constant temperature on the fine structure of a thermal plume.

2.1 Physical Configuration and Measurement Technique

The physical configuration under investigation is illustrated in Fig.1.a. It is mainly constituted of a rectangular hot obstacle (1) and a vertical channel (2). The channel open at the ends is the association of two parallel square Duralumin flats plates and two other rectangular Plexiglas plates. The height of the channel is L_2 = 40 cm and four distances between the Duralumin plates are considered 7.5 - b - 180 cm. Both plates are symmetrically heated at a uniform temperature of 323 K. At the channel entry is localized an obstacle heated only at the upper surface by joule effect at 573 K. This active source equidistant of two duralumin plates has a length of L_1 = 40 cm and a width of b_1 = 6 cm. The hot obstacle generates a thermal plume flow which interacts with thermosiphon flow inside the channel. The system is located on a frame (3) at 80 cm above the ground to allow air supply from below. A calibrated hot wire probe (4) is used to measure the fluctuations of temperature and velocity of the flow (Fig.1.b). The sensitive platinum wire of the probe has a diameter of D_f = 7.5 µm and a length of L_f = 3 mm. In this connection, the technique of a resistant wire anemometer at constant current (CCA) adopted in the present study has been discussed by many researchers (Brahimi *et al*., 1989; Naffouti *et al*., 2009; Son *et al*., 1975; Ben Maad and Belghith, 1992). A probe displacement system (6) in the x and z directions is used. A computer provided with a data acquisition card permits to save the instantaneous measurements of thermal and dynamic turbulent fields (5, 7, 8). After the application of Shannon theorem, the adopted sampling period is 15 ms. Owing to the strong dependence of the flow on the surrounding conditions, the experiment is carried out in a quiet atmosphere inside an independent closed room.

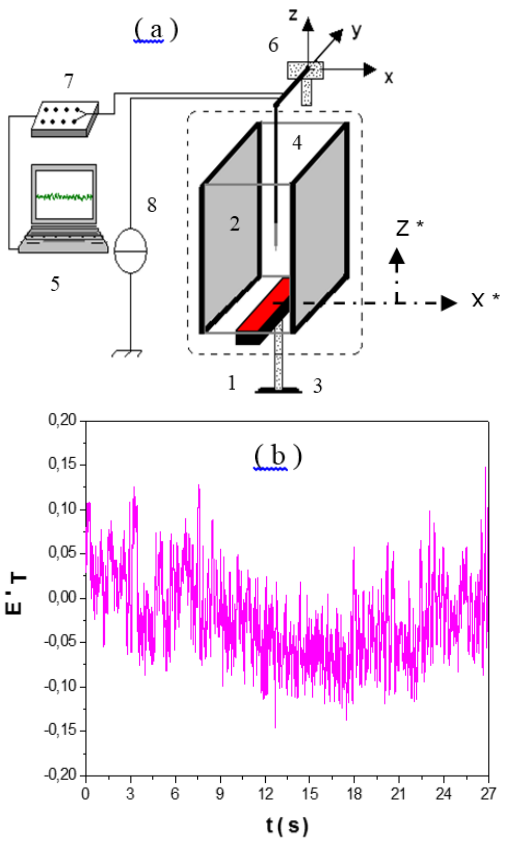

Fig. 1. Experimental setup (a) and irregular signal of temperature fluctuations sampled by the probe (b).

3. MAIN RESULTS AND DISCUSSIONS

Analysis of experimental data of thermal and dynamic fluctuations of the flow is carried out for a Rayleigh number equal to 0.63 10^7 and for air with Pr = 0.71. Four aspect ratios; A_1 = 1.25, A_2 = 1.83, A_3 = 2.5 and A_4 = 30 corresponding to spacing between channel walls; e_1 = 7.5 cm, e_2 = 11 cm, e_3 = 15 cm and e_4 = 180 cm, are examined. The Bohr effects are neglected and the physical problem is supposed 2D. Consequently, the thermal and dynamic fields are presented only on the mid-plane of channel (xOz). For each configuration, three sections are presented; Z* = 0.10, Z* = 0.37 and Z* = 0.92.

3.1 Aspect Ratio Effect of Channel on Thermal Turbulent Intensity

3.1.1 General View of Turbulent Field

The iso-values networks of thermal turbulent intensity reported to the temperature difference between the hot obstacle and the ambient air for various aspect ratios are illustrated in Fig.2. It is found that the turbulent field traced on the mid-plan of channel (xOz) is affected by the spacing between channel walls. For aspect ratio A_1, the figure shows the existence of two zones different from those of free thermal plume. Near the obstacle, a first zone is characterized by intense turbulence rate at X* = 0 owing to the predominance of the buoyancy forces. Higher than the hot source, the turbulence rates variation becomes relatively weaker thus indicating the establishment of turbulence in the second zone. Increasing aspect ratio to A_2, behavior of thermal turbulent field is completely changed. As we move away from the obstacle, turbulence rates decrease particularly at the upper region of channel due to the attraction of trapped threads aspired on both sides of active source by the hot walls. Consequently, the interaction between thermal plume and thermosiphon flow which surround it is feeble. For the configuration related to aspect ratio A_3, the structure of iso-values turbulent intensity is divided in three different zones. In the vicinity of the obstacle, a first zone is described by weak turbulence rates particularly on both sides of the obstacle. Downstream, an intermediate zone of pre-establishment of turbulence is characterized by the intensification of thermal turbulence in the central region of the flow due to a strong interaction between thermosiphon flow and thermal plume. A third zone where the variation of turbulent rates is weaker thus translating a better establishment of turbulence in the upper region of channel. A similar structure is given in the previous works (Ould Mohamed Mahmoud *et al*., 1998; Zinoubi *et al*., 2004) on the study of resulting flow of plume thermosiphon inside a vertical cylinder. For the highest aspect ratio A_4, it is found that the structure of thermal turbulent field is identical to the classical zones of a free thermal plume (Zinoubi *et al*., 2004). Consequently, the effect of thermosiphon flow is neglected for the case of channel walls far from the active obstacle.

3.1.2 Vertical Evolution of Turbulent Intensity

Standard deviation of thermal fluctuations obtained on mid-plane of canal (xOz) for X* = 0 at different aspect ratios is seen in Fig.3. Based on the observations of the plots, it is clear that the aspect ratio of canal affects the thermal turbulence. For smaller aspect ratio A_1, two different behaviors are identified as we move away from channel entry. Near the hot obstacle, the profile highlights a maximum of turbulence rate approximately at Z* = 0.05 related to a considerable interaction between the ambient air aspired by channel entry and the plume flow. For levels greater than Z* = 0.05, the turbulence rates decrease and their variation becomes relatively weak thus translating the establishment of turbulence. With increasing aspect ratio to A_3, thermal turbulence increases with the appearance of three different evolutions characterized by a maximum of turbulence rate near the level Z* = 0.2. This maximum corresponds to a significant effect of thermosiphon flow which interacts strongly with plume flow. For low levels Z* < 0.15, the weak values of turbulence rates are due to the preponderance of buoyant plume over thermosiphon flow close to active obstacle. For Z* > 0.2, a reduction of thermal turbulence versus Z* is observed. After, the turbulence remains constant beyond Z* = 0.6 thus indicating a fine establishment of thermal turbulence. Increasing aspect ratio to A_4, turbulent intensity decreases about 15 %. Regarding the results, we can suppose the existence of an optimum aspect ratio of channel characterized by a stronger turbulent intensity related to important effect of thermosiphon flow which favors a fast destruction of big vortices of thermal plume between vertical channel walls.

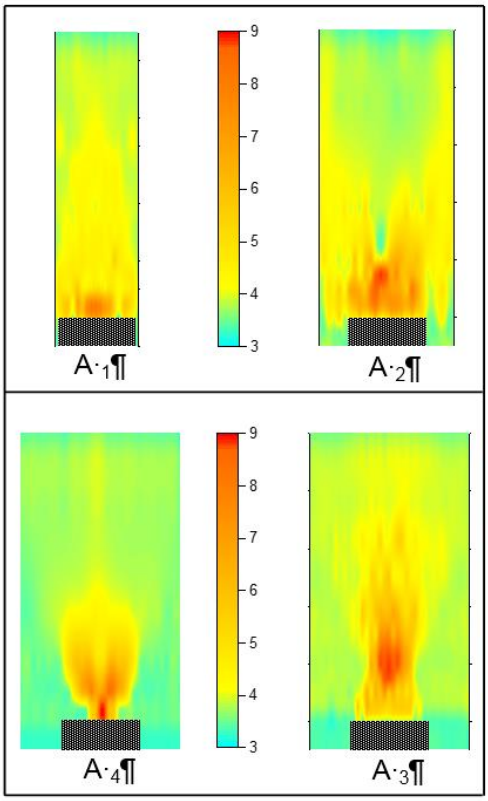

Fig. 2. General view of thermal turbulent intensity iso-values for various aspect ratio of the channel.

3.2 Aspect Ratio Effect of Channel on Dynamic Turbulent Intensity

3.2.1 Transversal Repartitions

Fig. 4 depicts the transversal repartition of dynamic turbulent intensity for three sections versus aspect ratio A ranging from A_1 = 1.25 to A_4 = 30. The plots show that the dynamic turbulent field is strongly influenced by the variation of the spacing between channel walls. For smaller aspect ratio A_1,

the profiles are flattened and the average value of dynamic fluctuations is about 20 % as we move away from the hot obstacle. This result demonstrates the preponderance of charge losses phenomenon which slows down the thermosiphon flow at channel entry. Increasing aspect ratio to A_3 causes an increase of turbulence rates above the active obstacle (Z* = 0.10) about 15 %. This growth is owing to a strong interaction between the buoyant plume and the supply puff coming from the channel entry. On both sides of the obstacle, turbulence rates are weaker due to the existence of a laminar flow of the thermosiphon. Downstream (Z* = 0.92), dynamic turbulence does not exceed 12 % and the fluctuations become comparable causing an establishment of turbulence in the higher region of channel. The same observations are presented by Naffouti *et al*. (2009, 2010) on the behavior of thermal plume evolving in a confined environment. For the largest aspect ratio A_4, plots present same evolution with a minimum of turbulence rates about 10 % owing to the preponderance of laminar aspect of thermal plume on mid-plane of channel (xOz). On both sides of the obstacle, a slight intensification of turbulence is observed as we move away from the active source.

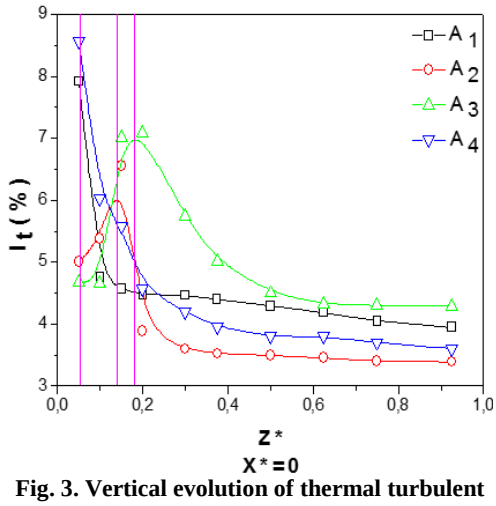

Fig. 3. Vertical evolution of thermal turbulent intensity for various aspect ratio of the channel.

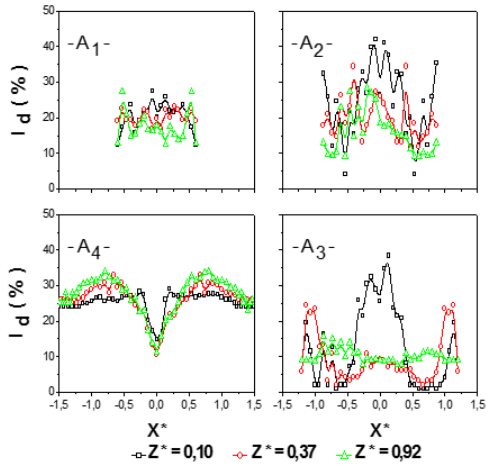

Fig. 4. Transversal distribution of dynamic turbulent intensity for three section vs various aspect ratio of the channel.

3.2.2 Vertical Evolution of Turbulence Intensity

Fig.5 illustrates the evolution of dynamic turbulence rates for X* = 0 with various values of aspect ratios of channel as a function of level Z*. The corresponding plots confirm that the structure of the flow is strongly affected by the variation of aspect ratio A. As it can be seen from the figure, the maximum of dynamic turbulence rate increases about 7 % with increasing aspect ratio from 1.25 to 2.5. This maximum which moves away from hot source versus aspect ratio consolidates the intensification of thermosiphon flow particularly for aspect ratio A_3. Beyond aspect ratio A_3, turbulence rates decrease and become comparable due to the absence of the thermosiphon phenomenon. From these analyses, it is possible to note the existence of an optimum aspect ratio characterized by significant dynamic turbulence rates.

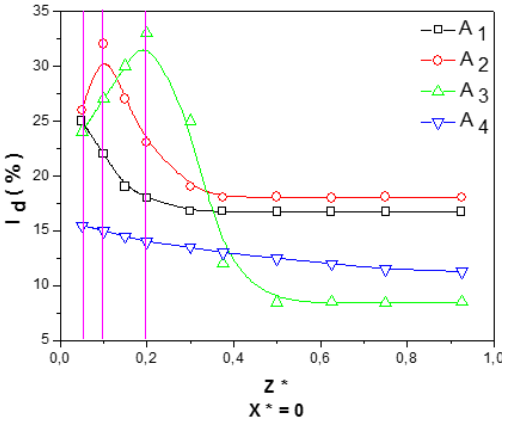

Fig. 5. Vertical evolution of the dynamic turbulence intensity for various aspect ratio of the channel.

3.3 Existence of an Optimum Aspect Ratio of Channel

Plots of the geometrical location of the maximum of thermal and dynamic turbulence intensity on the mid-plane of channel (xOz) versus aspect ratio are depicted in Figs. 6 and 7, respectively. The profiles consolidate the existence of an optimum aspect ratio observed previously by Naffouti *et al*. (2015) on the study of thermal and dynamic average fields of the flow. This optimum aspect ratio is near to 2.25 corresponding to aspect ratio A_3 (region 2) where the effect of thermosiphon is significant. It is characterized by a maximum of turbulence rate related to a strong interaction between thermal plume and thermosiphon flow. In region 1, the reduction of aspect ratio causes a weakening of thermal and dynamic turbulence thus indicating the preponderance of charge losses particularly for smallest aspect ratio A_1. For aspect ratios higher than optimum spacing (region 3), turbulence rates decrease with spacing between channel walls due to a weak interaction plume-thermosiphon in particularly for the biggest aspect ratio equivalent to free thermal plume.

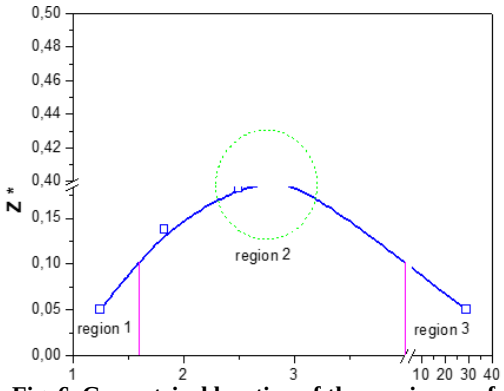

Fig. 6. Geometrical location of the maximum of thermal turbulence intensity on the mid-plane of channel (xOz) related to various aspect ratios.

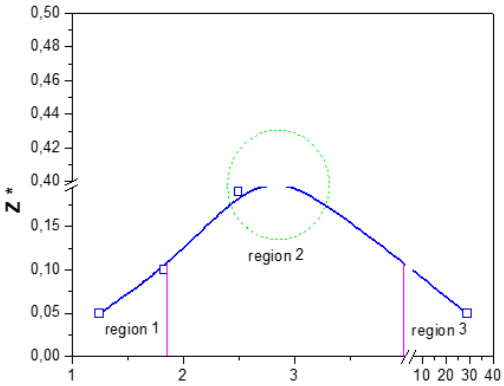

Fig. 7. Geometrical location of the maximum of dynamic turbulence intensity on the mid-plane of channel (xOz) related to various aspect ratios.

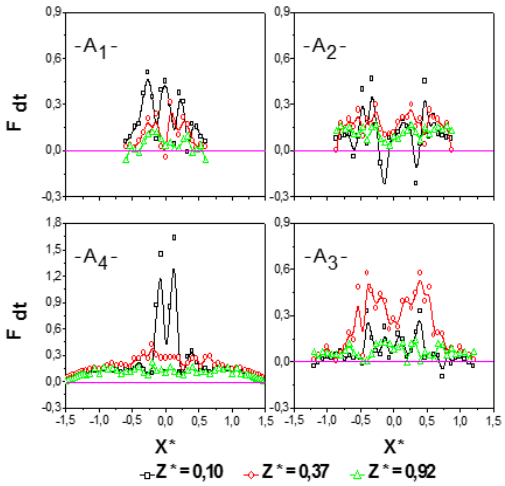

Fig. 8. Transversal evolution of thermal skewness factors vs aspect ratio of the channel for three sections.

3.4 Aspect Ratio Effect of Channel on Flatness and Skewness Factors

The transversal repartitions of thermal and dynamic skewness and flatness factors for three sections at various aspect ratios of channel are shown in Figs. 8-11. The analysis of these factors highlights the difference between the probability density law governing the fluctuations repartition of the fluid and the ideal Gaussian probability corresponding to the skewness and flatness factors $F_d = 0$ and $F_a = 3$, respectively. It is found that thermal and dynamic factors are strongly influenced by the changing of aspect ratio A.

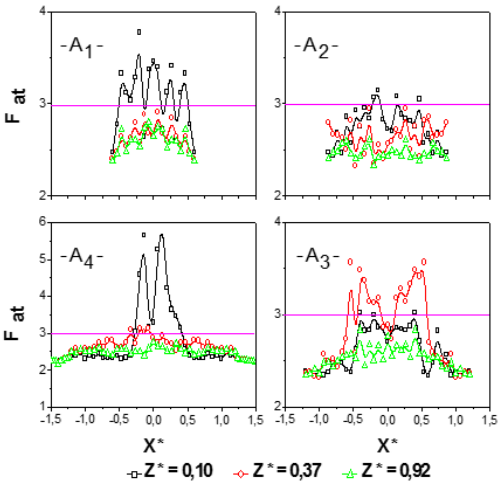

Fig. 9. Transversal evolution of thermal flatness factors vs aspect ratio of the channel for three section.

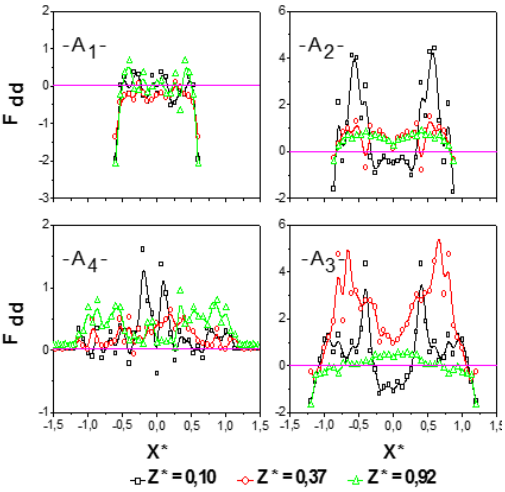

Fig. 10. Transversal evolution of dynamic skewness factors vs aspect ratio of the channel for three sections.

For aspect ratio A_1, figure 8 shows positive values of thermal skewness factors which decrease as we move away from the active obstacle. It is related to hot air puffs transported by the plume towards a region where the temperature is lower. Increasing aspect ratio to $A_3 = 2.25$, the values of skewness factors become practically zero at the end of channel ($Z^* = 0.92$) owing to an equiprobability of the existence of the plume and the supply air puffs. The negative skewness translates the preponderance of fresh air of thermosiphon flow which supplies the system by the low. For section $Z^* = 0.10$ just above the hot obstacle related to aspect ratio A_1, the values of thermal flatness factor are greater than 3 thus indicating the existence of the intermittency phenomenon between the plume flow and the

supply fresh air. For higher levels (Z* = 0.37 and Z* = 0.92), the flatness factors values become lesser than 3. On both sides of median plane of the obstacle and for aspect ratio A_3, the high flatness factors observed in section Z* = 0.37 are related to the considerable effect of thermosiphon flow which strongly interacts with thermal plume. Increasing aspect ratio increases the values of dynamic skewness and flatness factors (Figs.10 and 11) to attain its maximum on both sides of the hot obstacle for aspect ratio A_3 due to the intensification of thermosiphon phenomenon. Increasing aspect ratio to A_4, decrease these factors. For A_4, flatness factors are near to value 3 skewness factors are practically zero. Consequently, the repartition of flow fluctuations is similar to a Gaussian distribution far from the active source.

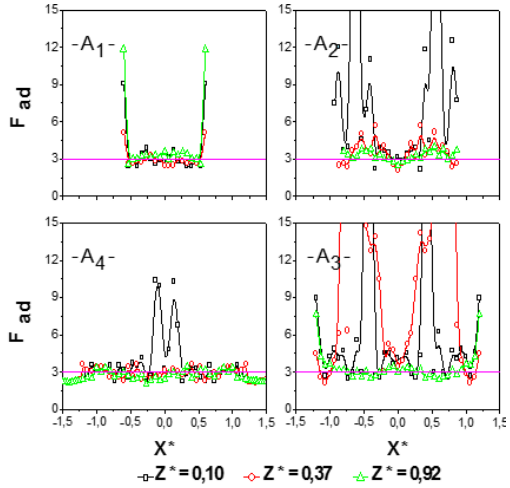

Fig. 11. Transversal evolution of dynamic flatness factors vs aspect ratio of the channel for three sections.

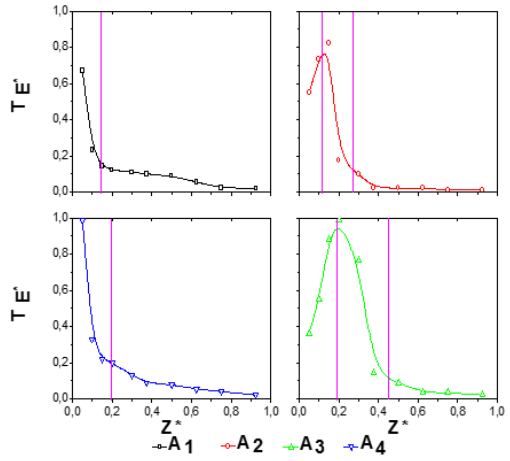

Fig. 12. Vertical evolution of the dimensionless turbulence thermal time scale vs aspect ratio of the channel for X* = 0.

3.5 Aspect Ratio Effect of Channel on Thermal Turbulence Scales

By integration temporal autocorrelation of thermal fluctuations, time integral scale is obtained using the following expression:

$T_E = \int_0^{t_0} R(\tau)\, d\tau$ where t_0 is the value which corresponds to R (τ) = 0.

Using the Taylor hypothesis (1977), length scale of turbulence is calculated by the following equation:

$L_E = T_E . V_0$ where V_0 is the average vertical velocity of the flow on the mid-plane of channel (xOz). The study of length scale of turbulence enables us to define the size of the vortices which characterize the development mechanisms of the flow turbulence inside the channel. Moreover, it defines the distance beyond those two fluid particles of the flow which cannot interact any more.

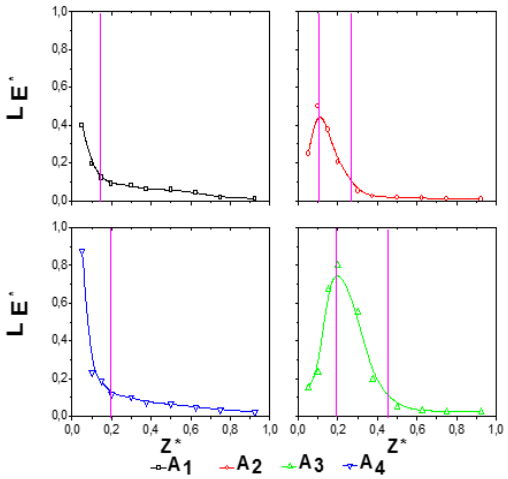

Fig. 13. Vertical evolution of the dimensionless turbulence thermal length scale vs aspect ratio of the channel for X* = 0.

The vertical evolution of time and length scales of thermal turbulence for various aspect ratios of channel and the height Z* on the median-plane of the obstacle (X* = 0) are plotted in Figs. 12 and 13, respectively. It is clear that both scales are affected by the changing of this geometrical parameter. For lower aspect ratio A_1, memory and length scale of turbulence decrease as we move away from the hot obstacle. This shows that the interaction between the vortices of the flow becomes feeble particularly at the channel exit where the dissipative vortices are predominant. For smaller aspect ratio A_1, the maximums of length and time scales are about 0.4 and 0.65 corresponding to 17 cm and 0.6 s, respectively. It is related to a strong interaction between the big scales generated by thermal plume and thermosiphon flow at channel entry. Increasing aspect ratio to A_3 = 2.5, memory and length scale of turbulence increase to attain its maximum about 0.98 and 0.74 corresponding to 9 s and 30 cm, respectively. Then, it decrease and the length scale is about a centimeter. For Z* = 0.2, the maximums confirm the strong effect of thermosiphon flow which interact strongly with thermal plume. For higher aspect ratio A_4, the evolution of thermal scale of turbulence is similar to smaller aspect ratio

A_1 and the length scale does not exceed 0.87 corresponding to 35 cm. Compared to several investigations on natural convection problems, the length scale obtained by; Agator and Son (1983) is 22.1 cm (free thermal plume), 10 cm (wall-plume), 11.5 cm (plume-plume) and Lochet *et al.* (1983) is 5.5 cm. The lenght scale for the dissipative vortices calculated by Dehmani *et al.* (1996) and Son (1977) is 0.9 cm and 1 cm, respectively.

3.6 Aspect Ratio Effect of Channel on Spectral Density of Thermal Fluctuations

In order to better characterize the fine structure of a turbulent flow, an analysis of the distribution of spectral energy of thermal fluctuations is necessary. In this study, we used the Fast Fourier Transform (FFT) proposed by Cooley and Tukey (1965). This technique is applied to autocorrelation function of temperature fluctuations $R(\tau)$ in order to obtain thermal spectra. In this connection, the FFT is adopted by many authors (Agator and Son, 1983; Lochet *et al.*, 1983; Cooley and Tukey, 1965; Ben.Maad and Belghith, 1994; Ould Mohamed Mahmoud *et al.*, 1998), on the problems of natural convection.

$$R(\tau)=\frac{\overline{T'(t).T'(t+\tau)}}{\sqrt{\overline{T'^{2}(t)}}.\sqrt{\overline{T'^{2}(t+\tau)}}}$$ where T' is the temperature fluctuation of the flow, t is the time parameter and τ is the time shift.

The spectra of thermal energy are standardized in the following form:

$\int_0^\infty E(n)\,dn=1$ where n indicate the frequency and E is the energy spectral density.

3.6.1 Logarithmic Presentation of Thermal Spectra

Profiles related to the normalized energy spectral density E of temperature fluctuations as a function of the frequency for various aspect ratio of channel and height Z* on median plane of active obstacle (X* = 0), are illustrated on Fig. 14. For each studied configuration, the increase of the frequency n leads to decrease the normalized amplitude. This behavior is consistent with the usual process of energy cascade from big vortices toward dissipative vortices. In fact, the main mechanism responsible for the energy cascade is the vortex stretching based on the elongation of vortex which enhances the thermal transfer between different vortices. Consequently, the viscous forces become intense and dissipate energy by the dissipative scales. In addition, the representation of these spectra in Log-Log coordinates consolidates the scenario of energy cascade by identifying some spectral laws known in natural convection. For lower frequency (0.1 - n - 8 Hz), law n^{-1} of Tchen (1953) is observed in raison to strong turbulent production of energy by big vortices created at channel entry (Z* = 0.10). Law n^{-3} introduced by Lumley *et al.* (1964), corresponding to the zone of transition towards turbulence (Z* = 0.37), is checked for intermediary frequency (8 - n - 15 Hz). It is related to vortices responsible of energy transfer from large structures to smaller scales. Law n^{-7} of Heisenberg (1977) corresponding to dissipative scales is showed at higher frequencies particularly for Z* = 0.92 where the viscous forces dominate the flow at channel exit. From this spectral analysis, it is found the absence of classical law $n^{-5/3}$ of Kolmogorov observed in forced convection owing to weak values of the Reynolds number of the flow.

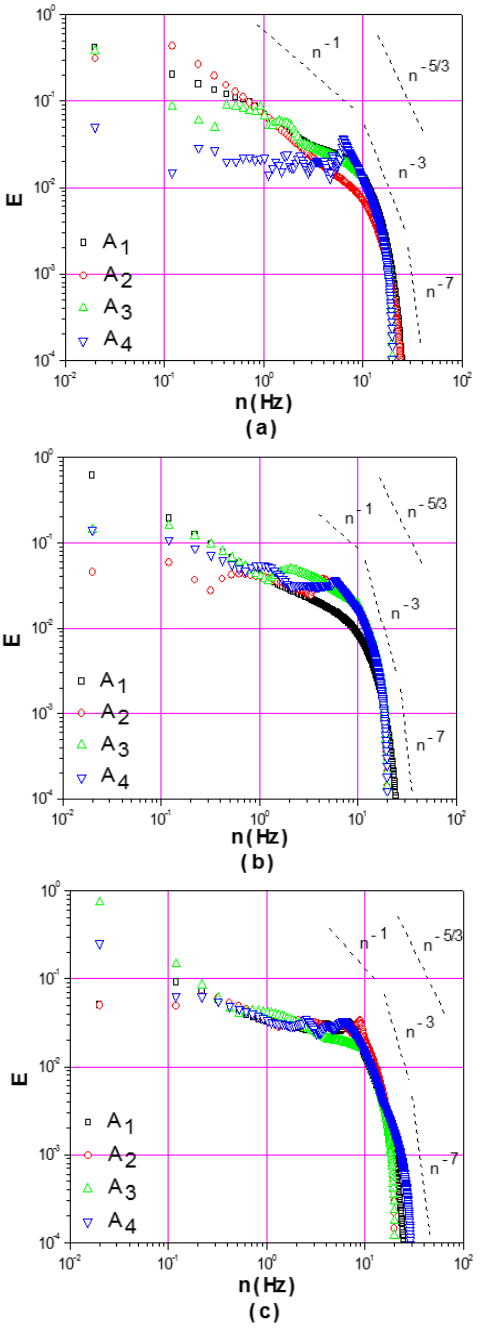

Fig. 14. Power spectral density of the temperature fluctuations vs aspect ratio of channel for X* = 0: (a) Z* = 0.10, (b) Z* = 0.37 et (c) Z* = 0.92.

3.6.2 Vertical Evolution of Spectral Density of Thermal Energy

Plots of the spectral density of thermal energy as a function of aspect ratio of channel and different height Z* for X* = 0 are depicted in Fig.15. This representation highlights the cascade of energy of the vortices particularly for aspect ratio A_3 corresponding to optimum energy transfer. The same process is found by Zinoubi *et al.* (2011) on the study of temperature spectra from a turbulent free thermal plume and in interaction with its material environment. For aspect ratio A_1, the profile consolidates the existence of two zones of the flow. Close to active obstacle, a first zone is characterized by a considerable production of energy owing to the predominance of the big vortices structures. Beyond Z* = 0.15, a second zone of energy transfer towards the small vortices. Increasing aspect ratio to A_3 = 2.5 changes the evolution of spectral density and consequently three different zones described previously are observed. A first zone near the obstacle (Z* < 0.10) is related to a strong production of energy by the large vortices which propagate from channel entry. For intermediary levels Z* corresponding to a reduction of spectral energy, the gap of the second zone of energy transfer towards the averages vortices increases with aspect ratio. This shows that the thermosiphon flow which strongly interact with thermal plume can favors the enhancement of heat transfer inside the canal by the destruction of the vortices structures. A similar trend is given in the previous investigations (Zinoubi *et al.*, 2004; Naffouti *et al.*, 2010). For higher Z*, a third zone of dissipative energy owing to the preponderance of dissipative vortices. For the greater aspect ratio A_4, the evolution of the profile is nearly identical to those of aspect ratio A_1 with an intensification of spectral energy near the obstacle.

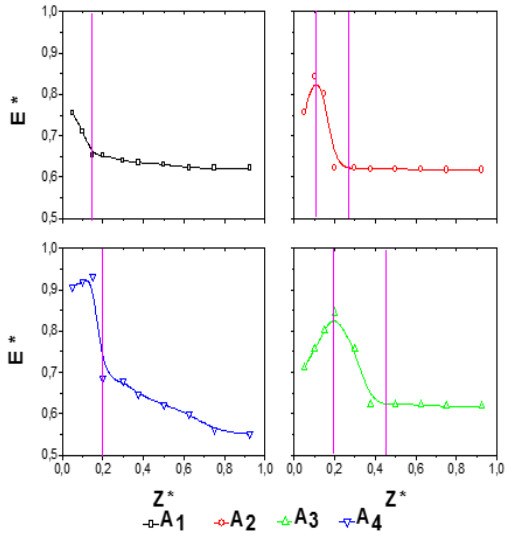

Fig. 15. Vertical evolution of power spectral density of the temperature fluctuations vs aspect ratio of channel for X* = 0.

4. CONCLUSION

The experimental investigation carried out in this article is a new contribution to analyze the effect of aspect ratio of a vertical channel on the turbulent characteristics of a thermal plume produced by an isothermal heat obstacle. This active source is localized at channel entry symmetrically heated at uniform temperature. To explore thermal and dynamic fluctuating fields between the hot walls of channel, the technique of hot wire anemometry at constant current (CCA) is used. The main results are illustrated as follows:

- It is concluded that the thermal and dynamic turbulent fields of the flow are strongly affected by the variation of the parameter aspect ratio of channel. For the smallest aspect ratio A_1, the structure of turbulent field is divided in two zones different from those of free thermal plume. Just above the obstacle, a first zone is characterized by strong turbulence rates. Higher, a second zone of established turbulence where the viscous forces are predominant. Increasing aspect ratio to A_3 completely changes the behavior of turbulent field and consequently a supplementary zone is observed close to the obstacle. This zone is characterized by weak thermal and dynamic fluctuations. Also, a growth of turbulence rates is detected downstream of the active obstacle owing to a significant effect of thermosiphon flow which strongly interacts with thermal plume. Increasing aspect ratio to A_4, the structure of thermal turbulent field becomes similar to that of free thermal plume and the dynamic turbulence intensity decreases about 15 %.

- It is shown the existence of an optimum aspect ratio of channel whose value is about A_3 characterized by maximum of thermal and dynamic turbulence rates and skewness and flatness factors owing to the intensification of thermosiphon phenomenon.

- Increasing aspect ratio to A_3, memory and length scale of turbulence in the vicinity of the active obstacle increase to attain its maximum about 9 s and 30 cm, respectively. Then, it decreases and the length scale is about 1 cm at channel exit. For aspect ratios A_1 and A_4, plots of turbulence thermal scale are similar and the length scale does not exceed 35 cm for higher aspect ratio.

- Spectral analysis shows a scenario of energy cascade of the vortices as we move away far from the obstacle to channel exit for different aspect ratio of channel. Some spectral laws known in natural convection are identified; laws of n-1 of Tchen, n-3 of Lumley and n-7 of Heisenberg related to big, average and dissipative vortices, respectively. Also, increasing aspect ratio to A3 favors the enhancement of heat transfer inside the channel by the destruction of the vortices structures with thermosiphon flow.

REFERENCES

Agator, J. M. (1983). Contribution à l'étude de la structure turbulente d'un panache thermique à symétrie axiale. Interaction du panache avec son environnement limité. Thèse de Docteur-Ingénieur, Université de Poitiers.

Agator, J. M. and D. K. Son (1983). Corrélation spatio-temporelle des fluctuations de température dans un panache thermique à symétrie axiale. Turbulence. *Comptes Rendus de l'Académie des Sciences*. Paris, t. (296).

Agator, J. M. and D. K. Son (1983). Analyse spectrale du champ thermique d'un panache turbulent à symétrie axiale. *Comptes Rendus de l'Académie des Sciences*. Paris, t. (296), 1119-1122.

Baum, R. T., K. B. McGrattan and M. R. Nyden (1998). An Examination of the applicability of computed tomography for the measurement of component concentrations in fire-generated plumes. *Combustion and Flame* (3), 358-372.

Maad, B. R. and A. Belghith (1992). The use of grid generated turbulence to improve heat transfer in passive solar systems. *Renewable Energy* (2), 333-336.

Maad, B. R. and A. Belghith (1994). The intensification of the heat transfer in passive solar systems using grid generated turbulence: spectral study. *Renewable Energy* (4), 319-325.

Bouslimi, J. and L. Dehmani (2005). Experimental investigation of the thermal field of a turbulent plume guided by a cylinder-preliminary results. *Experimental Thermal and Fluid Science* (29), 477–484.

Brahimi, M. (1987). Structure turbulente des panaches thermiques, Interaction. Thèse de Docteur en Physique, Université de Poitiers.

Brahimi, M., L. Dehmani and D. K. Son (1989). Structure turbulente de l'écoulement d'interaction de deux panaches thermiques. *International Journal of Heat and Mass Transfer* (32), 1551-1559.

Cheesewright, R. and D. K. Son (1978). Space time correlation measurement in a turbulent natural convection boundary layer. *International Journal of Heat and Mass Transfer* 21 (7), 911-921.

Cooley, J. W. and J. W. Tukey (1965). An Algorithm for the Machine Calculation of Complex Fourier Series. *Mathematic of Computation* (19), 297-301.

Debnath, R., A. Mandal, S. Majumder, S. Bhattacharjee and D. Roy (2015). Numerical Analysis of Turbulent Fluid Flow and Heat Transfer in a Rectangular Elbow. *Journal Applied Fluid Mechanics* (8), 231-241.

Dehmani, L. and D. K. Son (1996). Analyse spectrale du champ dynamique d'un panache turbulent rencontrant un milieu fortement stratifié. *International Communication in Heat and Mass Transfer* (23), 435-449.

Dehmani, L., D. K. Son and L. Gbahoué (1996). Turbulent structure of an axisymmetric plume penetrating a strong density stratification. *International Journal of Heat and Fluid Flow* (17), 452-459.

Dehmani, L. and M. Maalej (2002). Investigation of the self-similarity of a turbulent plume evolving in a stratified medium. *International Journal of Thermal Sciences* (41), 773–785.

Cortes, J. C. E. and C. Baudet (1999). Ultrasound scattering from a turbulent round thermal pure plume. *Experimental Thermal and Fluid Science*. (18), 271-281.

Cortés, J. C. E., R. Contreras, D. Boyer, M. Pavageau and R. H. Hernandez (2004). Temperature spectra from a turbulent thermal plume by ultrasound scattering. *Experimental Thermal and Fluid Science* (28), 803–813.

Haraa, T. and S. Katob (2004). Numerical simulation of thermal plumes in free space using the standard k-epsi model. *Fire Safety Journal* (39), 105–129.

Inard, C., A. Meslem, P. Depecker and P. Barles (1997). Structure moyenne et analyse intégrale du panache thermique des convecteurs électriques. *Revue Géneral de Thermique* (36), 495-509.

Lavrov, A., A. Utkin, R. Vilar and A. Fernandes (2006). Evaluation of smoke dispersion from forest fire plumes using lidar experiments and modelling. *International Journal of Thermal Sciences* (45), 848-859.

Lee, E. J., C. BoOh, K. Chul Oh, Y. H. Yoo and H. J. Shin (2010).Performance of the smoke extraction system for fires in the Busan–Geoje immersed tunnel. *Tunnelling and Underground space Technology Journal* (25), 600–606.

Li, A., Y. Zhang, J. Hu and R. Gao (2014). Reduced-scale experimental study of the temperature field and smoke development of the bus bar corridor fire in the underground hydraulic machinery plant. *Tunnelling and Underground space Technology Journal* (41), 95–103.

Lochet, R., D. Lemonnier and D. K. Son (1983). Correlation en convection naturelle turbulente. Influence de la pression et de la nature du gaz. *International Journal of Heat and Mass Transfer* (26), 1221-1227.

Lumley, J. L., H. A. Panofsky, J. Wiley and Sons (1964). *Journal of the Atmospheric Sciences* (21), 99-102.

McGrattan, K. B., H. R. Baum and R. G. Rehm (1996). Numerical simulation of smoke plumes from large oil fires. *Atmospheric Environment* (30), 4125-4136.

Naffouti, T., J. Zinoubi and R. B. Maad (2015). Experimental investigation of the effect of spacing between vertical plates on the development of a thermal plume from an active block. *Journal Applied Fluid Mechanics* (8), 75-84.

Naffouti, T., J. Zinoubi and R. B. Maad (2010). Experimental characterization of a free thermal plume and in interaction with its material environment. *Journal Applied Thermal Engineering* (33), 1632-1643.

Naffouti, T., J. Zinoubi and R. B. Maad (2013). Lattice Boltzmann Analysis of 2-D Natural Convection Flow and Heat Transfer within Square Enclosure including an Isothermal Hot Block. *International Journal of Thermal* Technology (3), 146-154.

Naffouti, T., M. Hammami, M. Rebay and R. B. Maad (2009). Experimental Study of a Thermal Plume Evolving in a Confined Environment: Application to Fires Problems. *Journal Applied Fluid Mechanics* (2), 29-38.

Naffouti T. and R. Djebali (2012). Natural convection flow and heat transfer in square enclosure asymetrically heated from below: A lattice Boltzmann comprehensive study. *Computer Modelling in Engineering and Science*s *Journal* (88), 211-227.

Ould, M. M. A. (1998). Etude de l'interaction d'un panache thermique à symétrie axiale avec un écoulement de thermosiphon. Thèse de Doctorat, Faculté des Sciences de Tunis.

Ould Mohamed Mahmoud A., R. B. Maad and A. Belghith (1998). Interaction d'un écoulement de thermosiphon avec un panache thermique à symétrie axiale: étude expérimentale. *Revue Géneral de Thermique* (37), 385-396.

Ould Mohamed Mahmoud A., R. B. Maad and A. Belghith (1998). Production of hot air with quasi uniform temperature using concentrated solar radiation. *Renewable Energy* (13), 481-493.

Pham, M. V., F. Plourde and S. D. Kim (2006). Effect of swirl on pure turbulent thermal plume development. *International Journal of Heat and Fluid Flow* (27), 502–513.

Porterie, B., N. Zekri, J. P. Clerc and J. C. Loraud (2007). Modeling forest fire spread and spotting process with small world networks. *Combustion and Flame* (149) (1-2), 63-78.

Rahmani, K., A. Bentebbiche and B. Draoui (2013). Numerical Investigation of Turbulent Natural Convection for a Cavity Having Sinusoidal Protuberances on a Vertical Wall. *Journal Applied Fluid Mechanics* (6), 491-499.

Rosdzimin, A. R. M., N. A. C. Sidik and S. M. Zuhairi (2010). Study of plume behavior two heated cylinders at high Rayleigh number using Lattice Boltzmann method. *The 10th Asian International Conference on Fluid Machinery* (1225), 780-787.

Shi, C. L., M. H. Zhong, T. R. Fu, L. He and R. Huo (2009). An investigation on spill plume temperature of large space building fires. *Journal of Loss Prevention in the Process Industries* (22), 76-85.

Shiraishi, Y., S. Kato, S. Murakami, S. Kim and R. Ooka (1999). Numerical analysis of thermal plume caused by large-scale fire in urban area. *Journal of Wind Engineering Industrial. Aerodynamics* (81), 261-271.

Son, D. K. (1977). Contribution à l'étude de la zone de transition et de la zone de turbulence établie dans un écoulement de convection naturelle sur une plaque plane verticale isotherme. Thèse de Doctorat d'Etat, Université de Poitiers.

Son, D. K., M. Stage and J. Coutanceau (1975). Transfert de chaleur entre un fil anémométrique court et un écoulement à faible vitesse. *Revue Géneral de Thermique* (168).

Tchen, C. M. (1953). On the spectrum of energy in turbulent shear flow. *Journal of Research of the National Bureau of Standards* (50), 51-62.

Wang, Y., J. Jiang and D. Zhu (2009). Full scale experiment research and theoretical study for fires in tunnels with roof openings. *Fire Safety Journal* (44), 339–348

Yang, H. Q. (1992). Buckling of a thermal plume. *International Journal of Heat and Mass Transfer*. (35), 1527-1532.

Yucel, N., M. I. Berberoglu, S. Karaaslan and N. Dinler (2008). Experimental and numerical simulation of fire in a scaled underground station. *Proceeding of World Academy of Science. Engineering and Technology* (40), 309.

Zinoubi, J., A. Gammoudi, T. Naffouti, R. B. Maad and A. Belghith (2007). Developpement of an Axisymmmetric Thermal Plume between Vertical Plates. *American* J*ournal Applied Sciences* (4), 679-685.

Zinoubi, J., R. B. Maad and A. Belghith (2004). Experimental study of the resulting flow of plume-thermosiphon interaction: application to chimney problems. *Applied Thermal Engineering*. (25), 533-544.

Zinoubi, J., R. B. Maad and A. Belghith (2004). Influence of the vertical source-cylinder spacing on the interaction of thermal plume with a thermosiphon flow: an experimental study. *Experimental Thermal and Fluid Science*. (28), 329-336.

Zinoubi, J., T. Naffouti and R. B. Maad (2011). Temperature Spectra from a Turbulent Free Thermal Plume and in Interaction with its Material Environment. *Journal Applied Fluid Mechanics* (4), 69-76.